



## Pharmaceutical Nanotechnology

## Chitosan-g-PEG nanoparticles ionically crosslinked with poly(glutamic acid) and tripolyphosphate as protein delivery systems

Sofia A. Papadimitriou, Dimitris S. Achilias, Dimitrios N. Bikiaris\*

Laboratory of Polymer Chemistry and Technology, Department of Chemistry, Aristotle University of Thessaloniki, 541 24 Thessaloniki, Greece

## ARTICLE INFO

## Article history:

Received 1 February 2012

Received in revised form 1 April 2012

Accepted 2 April 2012

Available online 10 April 2012

## Keywords:

Chitosan

Poly(ethylene glycol)

Bovine serum albumin

Poly(glycolic acid)

Tripolyphosphate

Nanoparticles

## ABSTRACT

In the present study chitosan grafted copolymers with poly(ethylene glycol) (CS-g-PEG) were prepared and studied using PEG with molecular weights 2000 and 5000 g/mol. The materials were characterized using  $^1\text{H}$  NMR, FTIR and WAXD techniques. These polyelectrolytes were ionically crosslinked with tripolyphosphate (TPP) and poly(glutamic acid) (PGA) at different polymer/crosslinking agent ratios (1:1, 2:1, 3:1 and 4:1, w/w) for the nanoencapsulation of bovine serum albumin (BSA). Prepared nanoparticles are spherical in shape with a mean diameter ranging from 150 to 600 nm. The size depends mainly to the molecular weight of the PEG and the crosslinking agent used. The PEG molecular weight also seems to affect the release rate of BSA especially the first burst effect which appears to be high in copolymers containing PEG5000, compared with copolymer prepared with PEG2000, and it is also higher when PGA was used as crosslinking agent, instead of TPP.

© 2012 Elsevier B.V. All rights reserved.

## 1. Introduction

Polymeric nanoparticles have been widely investigated as carriers for drug delivery using many different materials and methods for the preparation and size control (Rao and Geckeler, 2011). Among them, much attention has been paid to the nanoparticles that are made of synthetic biodegradable aliphatic polymers due to their good biocompatibility (Papadimitriou and Bikiaris, 2009). However, these nanoparticles are not ideal carriers for hydrophilic protein drugs because of their hydrophobic properties (Shu et al., 2009). In recent years, nanotechnology of polycation based materials is used in creating evolved drug delivery systems since it may offer site-specific and/or time-controlled delivery of small or large molecular weight drugs and other bioactive agents (Park et al., 2010; Howard, 2009). Besides the commonly used synthetic polymers, active research is focused on the preparation of nanoparticles using natural hydrophilic polymers like chitosan (CS). Chitosan has been largely favored as a potential nanoparticle carrier due to its unique properties (Dash et al., 2011; Hamidi et al., 2008; Liu et al., 2008). Despite the superiority of chitosan as biomaterial, it has the main drawback of poor solubility in water. However water soluble chitosan can be easily synthesized with proper chemical modification (Werle et al., 2009).

Chemical modification through graft copolymerization is quite promising as it provides a wide variety of molecular characteristics (Yao et al., 2007). The poly(ethylene glycol) (PEG) grafting of chitosan cope with the major problem of nanoparticles which is their rapid elimination from the blood stream through phagocytosis after intravenous administration and recognition by the macrophages of the mono-nuclear phagocyte system. PEGylation of chitosan nanoparticles can increase their physical stability and prolong their circulation time in blood by reducing the removal by the reticuloendothelial system. PEGylated chitosan nanoparticles have been investigated as nanocarriers (Yang et al., 2008). At the same time chitosan nanoparticles are usually prepared by ionic gelation method using tripolyphosphate (TPP). The ionic gelation method has received much attention in recent years for the preparation of nanocarriers for low molecular drugs (Papadimitriou et al., 2008). Recently some studies are referred to the use of TPP as ionic crosslinking agent for PEG-g-CS materials in order to create nanoparticles for encapsulation of macromolecular drugs (Zhang et al., 2008a; Csaba et al., 2009). Another technique is the creation of self-assembled polyelectrolyte complexes (PECs) which have been recently investigated for protein delivery (Park et al., 2010; Amidi et al., 2010). Oppositely charged polyelectrolytes can form stable intermolecular complexes. Recently poly(glutamic acid) is used as polyanion for the creation of PEC chitosan nanoparticles as protein delivery systems. (Tang et al., 2010; Keresztessy et al., 2009; Imoto et al., 2010; Peng et al., 2009). Poly(glutamic acid) is an unusual anionic, natural polypeptide, water soluble, biodegradable and edible and with its good tissue affinity gains interest for biological

\* Corresponding author. Tel.: +30 2310 997812; fax: +30 2310 997667.  
E-mail address: [dbic@chem.auth.gr](mailto:dbic@chem.auth.gr) (D.N. Bikiaris).

applications (Tsao et al., 2011). These kind of nanoparticles are prepared by electrostatic complexation of poly(glutamic acid) (PGA) and chitosan. PGA is selected as a negatively charged crosslinking agent as it has been shown that nanoparticles containing this polymer have the capacity to target hepatocytes (Lin et al., 2005).

Based on the aforementioned comments, the main idea of this study was to prepare modified chitosan nanoparticles as targeted and protection drug delivery systems for proteins. In an alginate/chitosan nanoparticle system, insulin was protected by forming complexes with cationic  $\beta$ -cyclodextrin polymers (CP $\beta$ CDs), which were synthesized from  $\beta$ -cyclodextrin ( $\beta$ -CD), epichlorohydrin (EP) and choline chloride (CC) through a one-step polycondensation (Zhang et al., 2010). Due to the electrostatic attraction between insulin and CP $\beta$ CDs, as well as the assistance of its polymeric chains, CP $\beta$ CDs could effectively protect insulin under simulated gastrointestinal conditions. In the present study in order to create drug carriers that will not be rapidly eliminated from the blood stream, poly(ethylene glycol) was used for the chemical modification of chitosan, creating graft copolymers. The materials produced were fully characterized and subsequently used as drug nanocarriers for the encapsulation of peptide/protein drug such as BSA. Nanoparticles were produced by the ionic gelation method using two different crosslinking agents, TPP and poly(glutamic acid). To our knowledge, no other research has been published until now referring to the use of poly(glutamic acid) as ionically crosslinking agent for CS-g-PEG materials, in order to create protein nanocarriers. The nanoparticles were fully characterized. Moreover the *in vitro* release of BSA from the nanoparticles was studied. The main goal of the present work was to identify the effect of the materials' ratio and crosslinking agent, together with the PEG molecular weight on the physicochemical characteristics of the CS-g-PEG/TPP and CS-g-PEG/PGA nanoparticles loaded with BSA. Therefore, the encapsulation efficiency, yield, drug loading were determined and release profile of BSA was also performed and studied.

## 2. Materials and methods

### 2.1. Materials

Chitosan with high molecular weight (MW: 350 000 g/mol, deacetylation degree >75% and viscosity 800–2000 cp) and tripolyphosphate were supplied by Aldrich chemicals. Monomethylated PEG (mPEG) with molecular weights 2000 g/mol (mPEG2000) and 5000 g/mol (mPEG5000), respectively, were supplied also by Aldrich chemicals. Poly(glutamic acid) (PGA) (average molecular weight 15 000–50 000 g/mol) and bovine serum albumin (BSA) were purchased from Sigma Aldrich and Acros Organics, respectively. All other materials and reagents used in this study were of analytical grade.

### 2.2. Preparation of PEG-aldehyde (mPEG-CH=O)

PEG-aldehyde was prepared, as previously reported in the literature, by the oxidation of PEG with DMSO/acetic anhydride (Harris et al., 1984; Sugimoto et al., 1998). For this reason 5 ml of acetic anhydride was added under  $N_2$  atmosphere to 32 ml anhydrous dimethylsulfoxide containing 10 g mPEG ( $\bar{M}_N = 2000$  g/mol) and 6%  $CHCl_3$  and the mixture was stirred for 9 h at room temperature (20 °C). The reaction mixture was then poured into 400 ml diethylether. The precipitate was filtered, dissolved in chloroform and reprecipitated twice by the use of diethylether. For the preparation of PEG-aldehyde two different molecular weights of mPEG were used, 2000 and 5000 g/mol.

### 2.3. Preparation of CS-g-PEG materials

The preparation of CS-g-PEG materials was performed by the method of Harris (Harris et al., 1984) which was partially modified by the use of novel synthetic procedures (Yao et al., 2007). CS (0.5 g) was dissolved in a mixture of aqueous 2% acetic acid solution (40 ml) and methanol (20 ml) and an aqueous solution of PEG-aldehyde (mPEG-CH=O) with MW = 2000 g/mol (2.9 g) was added dropwise during stirring for 30 min at room temperature (Sugimoto et al., 1998; Muslim et al., 2001). Then the pH of chitosan/PEG-aldehyde solution was increased by gradually adding  $Na_2CO_3$  until pH = 6. After 1 h  $NaCNBH_3$  (0.183 g) was added and the mixture was stirred for 5 h at 55 °C. The precipitate was obtained by pouring the reaction mixture into a saturated ammonium sulfate solution (Gorochovceva et al., 2005). The material was collected by filtering and dialyzed against aqueous 0.05 M NaOH and water alternately, for 96 h using a dialysis cellulose membrane bag (mw cut-off 12 400 g/mol), with a frequent change of the solutions used, until the pH of the external water phase reached 7. The material from the inner solution was freeze-dried and washed with ethanol and acetone in order to remove the remaining mPEG that did not reacted. After drying in vacuum the obtained white powder was CS-g-PEG.

### 2.4. Characterization of PEG-aldehyde and CS-g-PEG materials

#### 2.4.1. Nuclear magnetic resonance (NMR)

$^1H$  NMR and  $^{13}C$  NMR spectra of prepared materials were obtained with a Bruker AMX 400 spectrometer. Deuterated chloroform ( $CDCl_3$ ) was used as solvent in order to prepare solutions of 5% (w/v). The number of scans was 10 and the sweep width was 6 kHz.

#### 2.4.2. Fourier transform-infrared spectroscopy (FT-IR)

FTIR spectra were obtained using a Perkin-Elmer FTIR spectrometer, model Spectrum 1000. In order to collect the spectra, a small amount of each sample was mixed with KBr (1 wt% nanoparticles) and compressed to form tablets. The IR spectra of these tablets, in absorbance mode, were obtained in the spectral region of 450–4000  $cm^{-1}$  using a resolution of 4  $cm^{-1}$  and 64 co-added scans.

#### 2.4.3. Wide angle X-ray diffractometry (WAXD)

X-ray diffraction measurements of the samples were performed using an automated powder diffractometer Rigaku Mini Flex II with Bragg-Brentano geometry ( $\theta$ – $2\theta$ ), using  $CuK\alpha$  radiation ( $\lambda = 0.154$  nm) in the angle  $2\theta$  range from 5 to 55°.

### 2.5. Preparation of CS-g-PEG nanoparticles loaded with BSA

Nanoparticles were prepared by a simple ionic-gelation method. In this case the nanoparticles were self-assembled instantaneously upon addition of two different cross-linking agents an aqueous TPP or PGA in the presence of BSA into an aqueous CS-g-PEG solution under magnetic stirring at room temperature (Sonaje et al., 2010). In brief, aqueous CS-g-PEG (which was prepared using different molecular weights of PEG, PEG2000 or PEG5000) solutions at various concentrations, such as 0.5, 1, 1.5 and 2.0 mg/ml, were first prepared at pH = 3.5. Aqueous TPP or PGA (0.5 mg/ml final concentration) was premixed with BSA stock solution (2 mg final drug amount to the samples) and added into the aqueous CS-g-PEG solutions with a rate of 1 ml/min. The obtained nanoparticles (NPs) were collected by centrifugation at 32 000 rpm for 50 min. Supernatants were discarded and NPs were resuspended in deionized (DI) water for further studies.

## 2.6. Characterization of CS-g-PEG materials and nanoparticles

### 2.6.1. Morphological characterization of nanoparticles

Transmission electron microscopy (TEM) was used to examine the morphology of the nanoparticles prepared in this study. TEM micrographs of nanoparticle samples deposited on copper grids were obtained with a JEOL 120 CX microscope (Japan), operating at 120 kV.

The morphological examination of nanoparticles was also performed using a scanning electron microscope (SEM) type JEOL (JMS-840). Operating conditions were: accelerating voltage 20 kV, probe current 45 nA and counting time 60 s.

### 2.6.2. Size measurements of nanoparticles

The particle size distribution of CS-g-PEG/drug nanoparticles was determined by dynamic light scattering (DLS) using a Malvern Instrument (Worcestershire, United Kingdom) Zetasizer Nano ZS ZEN3600. This model is equipped with a 633 nm wavelength 'red' laser and a detector at 173° angle position measuring the non-invasive back-scatter with moving optics (NIBS is a patented technology). A suitable amount of nanoparticles was dispersed in distilled water (pH = 7) creating a total concentration 1% and was kept at 37 °C under agitation at 100 rpm.

## 2.7. Evaluation of drug encapsulation

The drug-loaded nanoparticles were centrifuged as described in previous paragraph and the amount of non-entrapped drug (free drug) was measured in the clear supernatant using UV spectrometry (Shimadzu PharmaSpec UV-1700) with Lowry method as described in the literature (Nikiforidis and Kiosseoglou, 2010; Markwell et al., 1978). The corresponding calibration curves were produced using the supernatant of blank nanoparticles. Each sample was measured in triplicate.

The drug loading capacity (LC) and association efficiency (AE) of the nanoparticles were calculated according to the following equations:

$$\%LC = \frac{\text{total drug} - \text{free drug}}{\text{nanoparticle weight}} \times 100 \quad (1)$$

$$\%AE = \frac{\text{total drug} - \text{free drug}}{\text{total drug amount}} \times 100 \quad (2)$$

## 2.8. In vitro drug release

BSA release was determined by incubating nanoparticles at 37 °C in phosphate buffer (pH = 7.4) under mild agitation. At pre-determined time intervals, samples were centrifuged and the supernatant was removed and replaced by fresh buffer. The amount of free BSA was determined by the method reported in the previous paragraph using UV-Vis spectrometry. In each experiment the samples were analyzed in triplicate.

## 3. Results and discussion

### 3.1. Synthesis and characterization of CS-g-PEG

Chitosan is a linear polysaccharide composed of randomly distributed  $\beta$ -(1–4)-linked D-glucosamine and N-acetyl-D-glucosamine. In its repeating unit it contains mainly hydroxyl and amino groups. However, these are very difficult to react at normal conditions with the hydroxyl end groups of PEG in order to prepare the grafted material (CS-g-PEG). Furthermore, in this case since PEG is a bifunctional reagent crosslinked macromolecules could be prepared. In order to avoid this mono methyl ether of PEG was used, which contains only one hydroxyl group in the

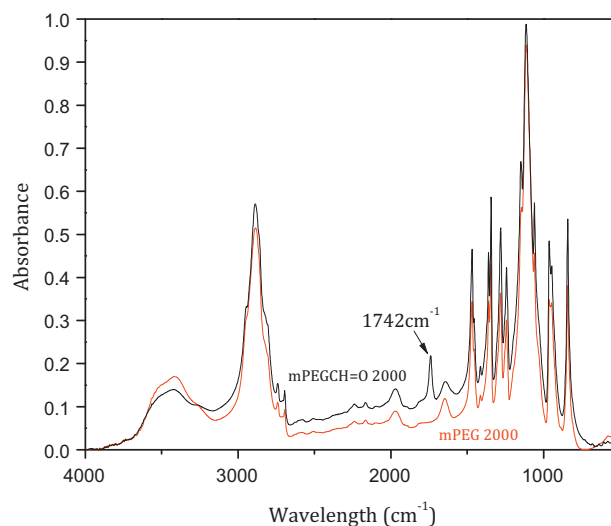


Fig. 1. FTIR spectra of (a) mPEG2000 and (b) mPEG-CH=O 2000.

macromolecular chain. To study the effect of PEG's molecular weight in the properties of the grafted material and mainly its behavior to BSA release, PEG having number average molecular weight,  $\bar{M}_N$ , 2000 and 5000 g/mol was used. Except this, for a successful grafting reaction of PEG into chitosan, PEG monomethyl ether was oxidized in a first stage to PEG-aldehyde with acetic anhydride and DMSO according to the method described by Sugimoto (Harris et al., 1984; Sugimoto et al., 1998). The room temperature was preferred for the oxidation reaction since there might be a chance of excessive reaction (Muslim et al., 2001). The creation of PEG-aldehyde was verified by the use of FTIR (Fig. 1). As can be seen the most characteristic peak to the spectrum of PEG-aldehyde is the one that appears at  $1742\text{ cm}^{-1}$ , which is ascribed to the aldehyde groups in which the hydroxyl end groups of PEG were transformed after the oxidation reaction.

After the successful synthesis of mPEG-CH=O with molecular weights 2000 and 5000 g/mol, PEG can be reacted with chitosan in order to prepare the grafted materials. The synthetic method used for the N-PEGylation of chitosan by the use of reductive amination is demonstrated in Fig. 2. One step-reductive amination, also known as Borch reduction, is the reaction between an amino group of a primary or secondary amines and aldehyde group in the presence of a reducing agent (Gorochovceva et al., 2005). Borch reaction requires a protic solvent or addition of an equivalent amount of an acid. Chitosan is soluble in acidic media and thus these conditions seem to be the most suitable for modification of chitosan. During the second step of the procedure, Schiff base is created and reduction reaction follows, leading to the CS-g-PEG graft copolymers. In both cases of the produced copolymers the reducing agent is added to the reaction mixture dropwise in a time period of 1 h in order to avoid precipitation of chitosan due to high alkalinity of  $\text{NaCNBH}_3$ . As previously reported the precipitation of chitosan during the reduction process of Schiff base by  $\text{NaCNBH}_3$  would suppress the smooth reduction of Schiff-base (Sugimoto et al., 1998). The excessive  $\text{NaCNBH}_3$  changes rapidly the pH of the solution from acidic to alkaline leading to the precipitation of chitosan in the aqueous solvent. The adjustment of pH to 6.5 with the use of  $\text{Na}_2\text{CO}_3$  before the reduction of Schiff base, leads to a smooth transfer of the pH from acidic to alkaline with the dropwise addition of  $\text{NaCNBH}_3$ , and consequently to the protection of chitosan from precipitation. Also neutral pH suppresses the degradation of Schiff-base (Yao et al., 1994).

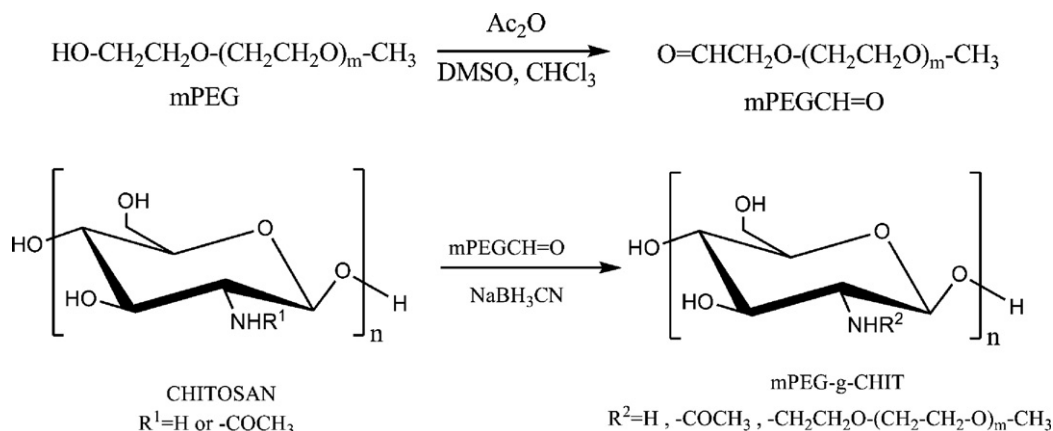


Fig. 2. Synthetic route via the two-step reaction for the synthesis CS-g-PEG.

During the grafted reaction it is possible some reagents and mainly mPEG-CH=O do not react with chitosan's amino groups. Separation and purification of the grafted copolymers is a rather complicated procedure. As previously reported (Sugimoto et al., 1998) the use of dialysis membrane is ineffective as a part of unreacted aldehyde of mPEG cannot be removed from the products. Having this in mind the salting out method was used (Gorochovceva et al., 2005). According to this technique the grafted copolymers created a concentrated gel-like upper phase under salting out and unreacted mPEG-CH=O remained in the solution. Finally the materials were dialyzed against water to remove the residual ammonium sulfate used for the salting out method.

Grafting of mPEG aldehyde on chitosan was confirmed by the use of FTIR spectroscopy. Comparative IR spectra of chitosan, mPEG5000 and the synthesized mPEGCH=O and CS-g-PEG are shown in Fig. 3.

To the spectra of grafted chitosan the characteristic peaks of chitosan and mPEG can be identified. The characteristic peaks of PEG at  $1110\text{ cm}^{-1}$  (C–O stretch) and  $2886\text{ cm}^{-1}$  (C–H stretch) appear more intense than those of chitosan at the grafted materials. Chitosan characteristic bands appear at  $3420\text{ cm}^{-1}$  (O–H stretch overlapped with N–H stretch) and  $2879\text{ cm}^{-1}$  (C–H stretch). On the contrary other two characteristic peaks of chitosan at  $1650\text{ cm}^{-1}$  and  $1560\text{ cm}^{-1}$ , that correspond to Amide I and Amide

II, respectively, show a quite different behavior. The absorbance of Amide I, at  $1650\text{ cm}^{-1}$ , seems to remain unaffected, a fact that seems to be reasonable as this peak is attributed to the stretching vibration of the C=O group of the acetylated amino groups of chitosan, which is not affected during the modification procedure of chitosan. Contrary the absorbance of Amide II,  $1560\text{ cm}^{-1}$ , is almost disappeared from the spectra of the grafted chitosan. This characteristic group is attributed to the bending vibration of N–H group of chitosan ( $\text{NH}_2$ ), and this constitutes strong evidence of the extend degree of reaction between the free  $\text{NH}_2$  groups of chitosan and the aldehyde group of mPEGCH=O (Bhattarai et al., 2005).

Typical XRD patterns of (a) mPEG5000 and (b) mPEG-CH=O 5000, (c) chitosan, (d) CS-g-PEG5000 are shown in Fig. 4. XRD pattern of neat CS showed that is in an amorphous to partially crystalline state. This observation is in accordance with Nunthanid (Nunthanid et al., 2001) who reported a peak at approximately  $10^\circ$  ( $2\theta$ ) corresponding to hydrated crystals and one at  $18^\circ$  ( $2\theta$ ) corresponding to anhydrous crystals. On the other hand the XRD pattern of mPEG5000 has two strong characteristic crystalline peaks at  $2\theta$  deg  $19.3^\circ$  and  $23.6^\circ$  and two weak crystalline peaks at  $2\theta$  deg  $26^\circ$  and  $27^\circ$ . CS-g-PEG5000 pattern gives also two obvious peaks that seem to be the characteristic peaks of mPEG but broadened due to

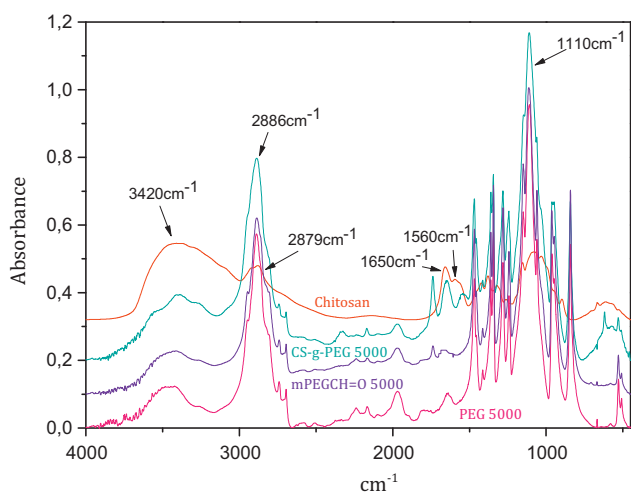


Fig. 3. FTIR spectra of (a) mPEG 5000, (b) mPEGCH=O 5000, (c) CS-g-PEG 5000 and (d) chitosan.

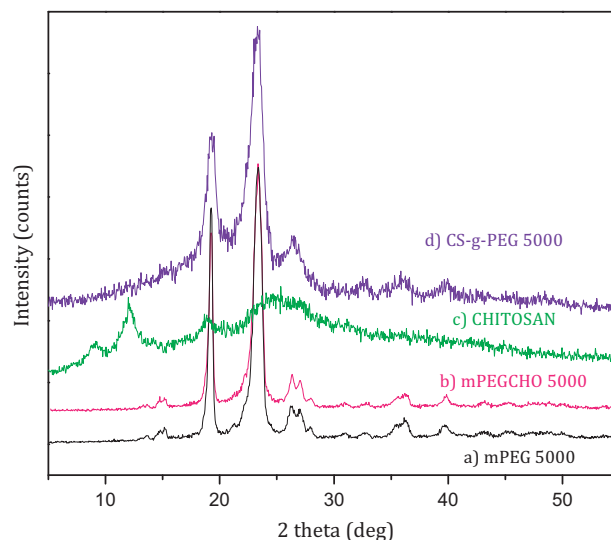


Fig. 4. X-ray powder diffraction patterns of (a) mPEG5000, (b) mPEGCH=O 5000, (c) chitosan and (d) CS-g-PEG5000.



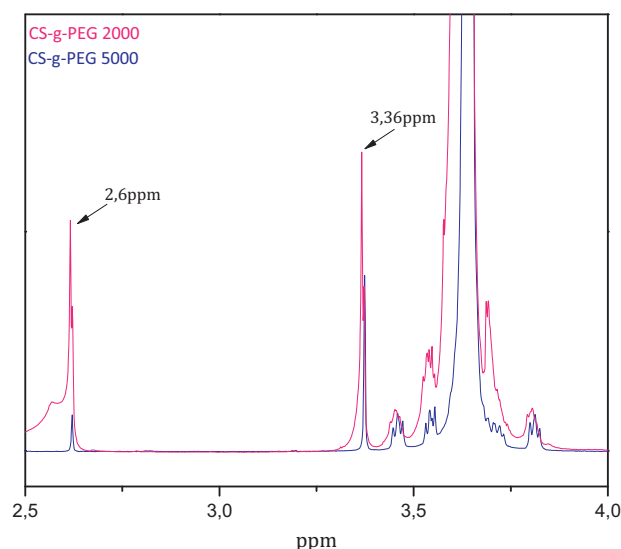


Fig. 5.  $^1\text{H}$  NMR spectra of CS-g-PEG2000 and CS-g-PEG5000.

the disrupt of PEG crystalline structure from amorphous chitosan (Deng et al., 2007)

The characterization of the grafted materials is completed through the  $^1\text{H}$  NMR spectra in order to calculate the degree of substitution (DS) of mPEG moiety (Yang et al., 2008). The characteristic proton signals of CS-g-PEG appeared in the range of 3.5–4.0 ppm (Fig. 5). The peak at around 3.36 ppm is attributed to the proton signal of methoxyl of CS-g-PEG and therefore the DS could be calculated by comparing the ratio of mPEG protons at 3.36 ppm to chitosan protons around 2.6 ppm (CH carbon 2 of glucosamine ring). The DS could be calculated by the following equation:

$$\text{DS} = \frac{I_{3.36\text{ppm}}}{3 \times I_{2.6\text{ppm}}} \times 100\% \quad (3)$$

According to this equation and the  $^1\text{H}$  NMR spectra it was found that the DS of mPEG moiety was 43% and 75% for CS-g-PEG with PEG2000 and PEG5000, respectively.

### 3.2. Preparation and characterization of CS-g-PEG nanoparticles loaded with BSA

Grafted chitosan materials were synthesized as shown above, in order to be used as a vehicle for the delivery of drugs through the formation of polyion complex. These materials are composed of a water soluble hydrophilic mPEG side chain and a cationic chitosan main chain. The mPEG side chain endows the chitosan molecule with increased solubility and has functional advantages such as the avoidance of the reticuloendothelial system (RES) and protein adsorption (Jeong et al., 2006).

In the present study, nanoparticles were prepared by a novel inter-ionic gelation method in aqueous medium (pH=3.5) and particles were obtained spontaneously during the process. Ionic interaction between the positive charge ions of the amino groups in chitosan and the negative charge groups of TPP or PGA can lead to the formation of inter-ionic polymer complexes. Polyionic hydrogels prepared by ionic gelation have the advantage of creating an ionic environment that favors the stabilization of bioactive agents as previously reported (Zhang et al., 2008a). During the process of nanoparticle preparation it was chosen the BSA to be in the same solution with the crosslinking agent and this solution to be added to CS-g-PEG as previous studies having reported that in this way smaller particle can be obtained and the size distribution of

these systems tends to be narrowest (Hajdu et al., 2008). Also is very important the pH that is being used during the preparation of nanoparticles especially in the samples where PGA is used as crosslinking agent. In our case it was chosen to be pH=3.5 and this is because the pKa values of the amino groups of chitosan and the carboxyl groups of PGA are approximately 6.5 and 2.9, respectively. In this range chitosan and PGA are ionized and consequently capable to form polyelectrolyte complexes, which result in a matrix structure with a spherical shape (Sonaje et al., 2010).

In Table 1 are demonstrated the nanoparticle samples that were produced. In the first column is demonstrated the name used for each sample (where the numbers 0.5, 1.0, 1.5 and 2.0 correspond to the final concentration mg/ml of the grafted chitosan to the sample) while in the second column is demonstrated the weight ratio of the grafted material to the crosslinking agent in the final sample. Also in Table 1 are summarized the results of the nanoparticle yield, the size of the prepared nanoparticles, the loading capacity and association efficiency of the grafted copolymers of chitosan. The  $\pm$  values denote the standard deviation between the measurements of the same sample (i.e. measurements error). These parameters mainly depend on the polymer nature and physicochemical characteristics of the model drug used as well as from the probable interactions between the polymer matrices, the crosslinking agent and the drug.

From Table 1 and the nanoparticle sizes that were measured by dynamic light scattering (DLS) many different and quite interesting results may arise. The mean diameter varied from 170 to 640 nm. All nanoparticle samples show a unimodal size distribution. It is observed that in all samples as the ratio of grafted polymer to crosslinking agent increases, which means the less crosslinking agent is used, the nanoparticle size seems to increase. Consequently it may be stated that the crosslinking agent, regardless of its nature small molecule like TPP or macromolecule like PGA, creates ionic interactions with the amino groups of chitosan which leads to a more compact and stable conformation for CS-g-PEG nanoparticles. In case of the samples A and B where TPP is used as the crosslinking agent, seems that the ratio of CS-g-PEG:TPP 2:1 gives the smaller nanoparticle sizes. On the contrary when PGA is used as crosslinking agent the nanoparticle size seems to increase with a decrease of the degree of crosslinking without any exceptions. Also the molecular weight of PEG seems to play an important role on the nanoparticle size. Thus, in the samples with the same kind and amount of crosslinking agent but with a different length of PEG chain grafted on chitosan (samples A with B and C with D) it can be stated that the nanoparticles created with a shorter PEG chain give smaller nanoparticle size. This is reasonable and expected as it is attributed to the core-shell structure that the grafted chitosan materials are able to create during the nanoparticles' preparation. It is likely that PEG covers the chitosan core to form a shell, since the PEG end-group migrates to the surface of nanoparticles during procedure, particularly because of the hydrophilicity of PEG (Zhang et al., 2008a). The higher molecular weight of PEG leads to longer PEG grafted chains resulting in bigger outer shell and hence size of the nanoparticles. This observation is reinforced by the fact that DS of CS-g-PEG 5000 is 75% unlike DS of CS-g-PEG 2000 which is 43%, giving to CS-g-PEG 5000 a bigger size and a more "stealth" character. Also it is observed that nanoparticle yield for all samples lies in a quite satisfactory level, 64–80%. Moreover, use of TPP as crosslinking agent results in high yield but with no significant and definite correlation in terms of the yield sequence values and the degree of crosslinking. When PGA is used, it can clearly be stated that there is an increase in nanoparticle yield despite the decrease of the degree of crosslinking. If the above mentioned results are combined with the values of loading capacity and association efficiency, it can be stated that the decrease of crosslinking degree with the use of PGA gives space to BSA in order to be encapsulated more efficiently in CS-g-PEG nanoparticles. BSA ( $I_p=4.7$ ) is

**Table 1**

Concentration and characteristics of BSA-loaded CS-g-PEG nanoparticles.

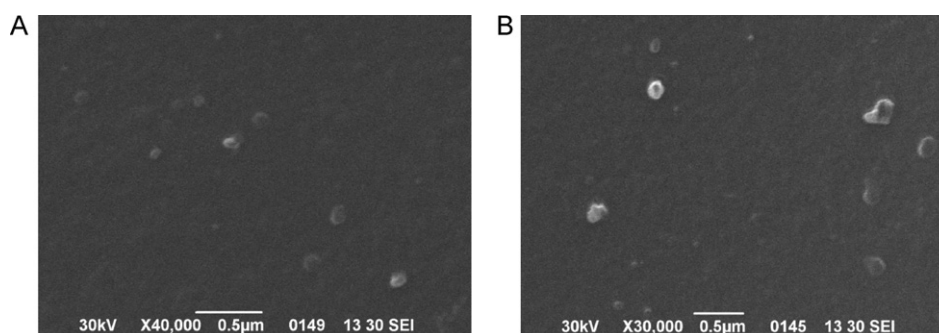
Sample code	CS-g-PEG2000/TPP (w/w)	Yield	Diameter (nm)	Loading capacity (%)	Association efficiency (%)
A2000 0.5	1:1	82.2 ± 2.5	382 ± 3	6.20	79.0
A2000 1.0	2:1	74.5 ± 2.9	177 ± 7	3.39	55.5
A2000 1.5	3:1	79.2 ± 2.6	309 ± 8	2.73	57.5
A2000 2.0	4:1	82.1 ± 0.4	328 ± 5	2.93	74.5
	CS-g-PEG5000/TPP (w/w)				
B5000 0.5	1:1	79.5 ± 2.4	554 ± 7	2.61	64.5
B5000 1.0	2:1	77.6 ± 1.4	497 ± 9	4.49	44.0
B5000 1.5	3:1	79.8 ± 1.5	541 ± 5	4.36	62.0
B5000 2.0	4:1	84.0 ± 3.8	609 ± 4	2.45	92.0
	CS-g-PEG2000/PGA (w/w)				
C2000 0.5	1:1	54.8 ± 2.9	304 ± 6	8.77	51.0
C2000 1.0	2:1	63.4 ± 0.8	456 ± 8	8.52	69.5
C2000 1.5	3:1	68.4 ± 2.5	562 ± 8	5.92	64.0
C2000 2.0	4:1	67.8 ± 6.3	643 ± 9	6.46	84.0
	CS-g-PEG5000/PGA (w/w)				
D5000 0.5	1:1	60.0 ± 5.8	400 ± 6	8.75	56.5
D5000 1.0	2:1	64.2 ± 1.5	401 ± 6	7.60	63.5
D5000 1.5	3:1	65.5 ± 3.2	525 ± 5	8.39	90.0
D5000 2.0	4:1	71.7 ± 1.7	521 ± 5	7.21	92.0

negatively charged at the pH that the experiment of nanoparticle manufacture takes place (pH = 3.5) which favors its electrostatic interaction with the positively charged amino groups of chitosan. If the Ip of protein is different, e.g. the protein is positively charged at the crosslinking reaction condition, the LC, AE and consequently release profiles should be quite different. In this case it is expected a lower value for LC and AE as the possible electrostatic interaction will appear weak (or even no interaction will be possible between chitosan and BSA) and unable to form strong interactions with the polymer matrix and eventually create well defined nanoparticles capable of protecting the active agent (BSA). At the same time release profile would be also quite different as it would be expected to give a significant burst effect at pH value 7.4 for drug release.

Scanning electron microscopy (SEM) and transmission electron microscopy (TEM) photographs from different nanoparticle samples are shown in Figs. 6 and 7. These images are also representative for the rest of the samples. SEM micrographs established that the BSA-loaded nanoparticles of CS-g-PEG copolymers had a discrete spherical shape with sizes ranging from 200 up to 300 nm, a fact that is not in agreement with the measurements of dynamic light scattering shown in Table 1. The size of the nanoparticles based on the TEM micrographs was about 100 nm or more, smaller than the size determined by DLS. This was mainly due to the process involved in the preparation of the sample and it could have been expected since the nanoparticles were dispersed in an aqueous phase for the DLS experiments, and chitosan has the ability to swell in contact with water, PEG is water soluble polymer and CS-g-PEG materials are also soluble in water, while the TEM experiments were

performed in dry samples (Aktas et al., 2005; Papadimitriou et al., 2008). Therefore the size determined by laser light scattering was a hydrodynamic diameter and was larger than the size measured by TEM because of solvent effect as previously reported (Yang et al., 2008).

In Fig. 8 XRD patterns of the prepared BSA loaded nanoparticles are presented. As can be seen, BSA is completely amorphous due to the absence of any characteristic peaks. In CS-g-PEG/BSA loaded samples the characteristic peaks of CS-g-PEG are recorded, which however in all samples are broadened, in comparison with the patterns of the neat materials. Furthermore, these peaks have lower intensity, a fact that justifies that the crystal structure of grafted materials is disrupted probably due to the electrostatic interactions that have been developed between the positively charged amino group of CS-g-PEG materials and the negative charged groups of the crosslinking agents TPP and PGA as previously reported (Lin et al., 2007). Also is obvious that when PGA is used as crosslinking agent (samples D and C) the intensity of the two characteristic peaks of CS-g-PEG materials is decreased even more in comparison with the samples where TPP is used as crosslinking agent (samples A and B). This may indicate that the intermolecular interactions between PGA-COO<sup>-</sup> groups and -NH<sub>2</sub><sup>+</sup> or -NH<sup>+</sup> groups of grafted chitosan may be stronger leading to a greater disrupt of the crystalline structure. At the same time the XRD patterns of BSA nanoparticles prepared with the grafted polymers, where the molecular weight of PEG is 5000 g/mol, show that the crystallinity is not affected as much as in case of the nanoparticle samples of CS-g-PEG where PEG molecular weight is 2000 g/mol. This may come as a result of the different degree of substitute of the two grafted

**Fig. 6.** SEM micrographs of CS-g-PEG nanoparticles (A) A2000 1.0 and (B) C2000 0.5.

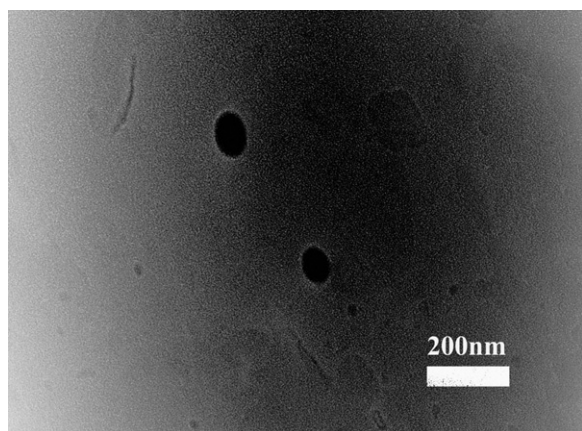


**Fig. 7.** TEM image of CS-g-PEG loaded BSA nanoparticles of the sample A2000 1.0.

materials and as it was calculated above is lower in PEG2000 (43%) compared with PEG5000 (75%).

In Figs. 9–12 is demonstrated the in vitro release profile of BSA protein from nanoparticles. In all cases the overall release process can be characterized as a biphasic procedure.

The initial burst effect, for all samples, in the first almost 5 h, varies between 10 and 30% of the encapsulated BSA. This burst effect may be attributed to the desorption of the protein close to the surface during preparation of the nanoparticles, which then diffused rapidly when the nanoparticles came into contact with the release medium, as previously reported (Zhang et al., 2008a). Also the surface of nanoparticles is consisted of PEG, which is water soluble and this contributes to the observed initial burst effect. Furthermore the rate of BSA release is affected by the PEG molecular weight. After the burst release period, the rate of release fell as the dominant release mechanism was changed to drug diffusion through chitosan matrix as previously reported (Papadimitriou et al., 2008). Furthermore BSA was released slowly due to swelling or degradation of the polymer. The remaining BSA in nanoparticles was not completely released until the particles were completely eroded or dissolved in release medium, which might have been due to the interaction between the remaining BSA and the few free

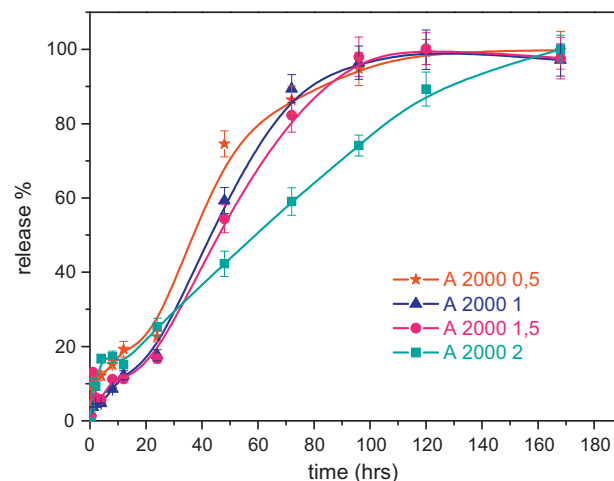


**Fig. 9.** The in vitro release profile of BSA from CS-g-PEG nanoparticles with PEG MW 2000 and TPP as ionic crosslinker (sample A).

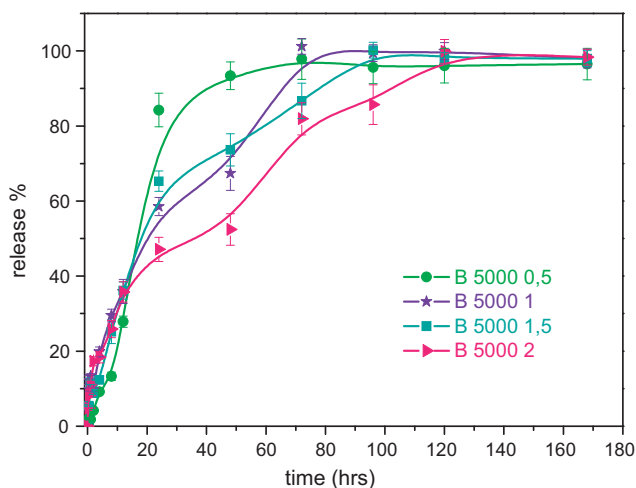


**Fig. 10.** The in vitro release profile of BSA from CS-g-PEG nanoparticles with PEG MW 5000 and TPP as ionic crosslinker (sample B).

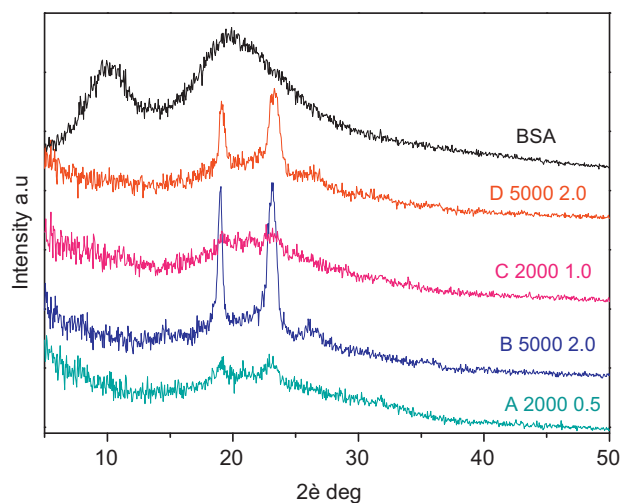


**Fig. 8.** X-ray powder diffraction patterns of BSA and CS-g-PEG loaded nanoparticles ionically crosslinked with TPP and PGA.

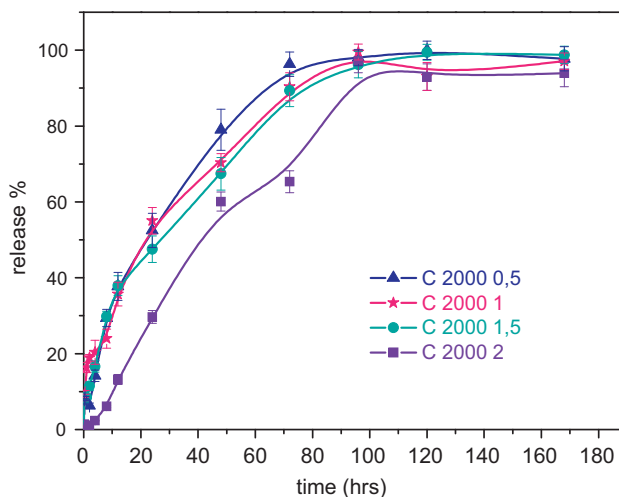


**Fig. 11.** The in vitro release profile of BSA from CS-g-PEG nanoparticles with PEG MW 2000 and PGA as ionic crosslinker (sample C).

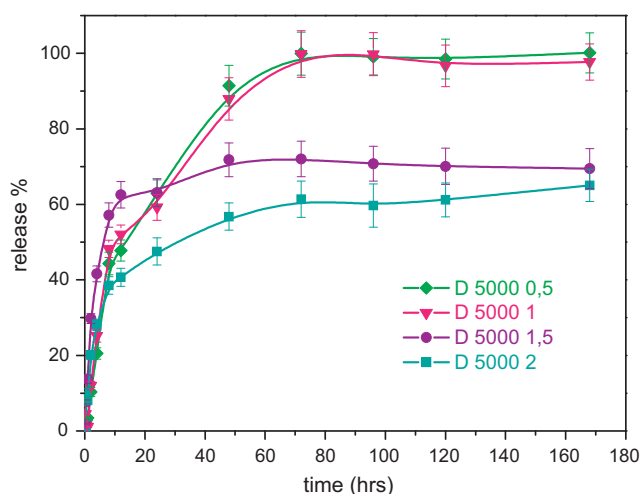


**Fig. 12.** The in vitro release profile of BSA from CS-g-PEG nanoparticles with PEG MW 5000 and PGA as ionic crosslinker (sample D).

amino groups on the chitosan segments (Zhang et al., 2008a,b) as it is previously established from the shift of the characteristic peaks in FT-IR spectra, mentioned above. At this point we have to point out that the different DS of CS-g-PEG 2000 and 5000 plays also its role in drug release of BSA. It is logically expected that CS-g-PEG 5000 would give a more intense burst effect as the DS of this material is 75%. Moreover, it is important to be stated that it is not possible to control the DS for these materials, as previously reported, in order to have exactly the same materials, with the same DS (Muslim et al., 2001; Gorochoveva et al., 2005; Sugimoto et al., 1998).

Except molecular weight of PEG the crosslinking agents play also an important role to the release behavior of BSA. When TPP is used as ionic crosslinker the release of BSA from nanoparticles seems to be slower (samples A and B, Figs. 9 and 10) toward the results obtained when PGA is used as crosslinking agent (samples C and D, Figs. 11 and 12). Probably this occurs because of the smaller molecular size of TPP, in comparison with PGA. Thus TPP has the ability to penetrate easily through the macromolecular chains of CS-g-PEG, during the nanoparticle formation, creating a more stable network of ionic interactions among the polymer matrix and the crosslinking agent. The aforementioned behavior may also be attributed to the low loading capacity of nanoparticles with TPP as it is shown in Table 1, which means that a lower amount of BSA exists to the outer surface of the nanoparticles and thus the release mainly occurs as a procedure of diffusion from the inner part of the nanoparticles rather than from the surface. Due to these differences it can be said that TPP may have higher efficiency as crosslinking agent, compared with PGA.

Another characteristic of these release profiles is that as the ratio of crosslinking agent is increased, independently TPP or PGA is used; the release rate seems to increase. This may be attributed to the fact that the less extent the ionic crosslinking of CS-g-PEG is, the more are the free amino groups of chitosan that can interact with the negative charged groups of BSA. As has been previously reported the reason for the slow drug release from the polyion complex micelles might be the strong ion complex between the amino group of chitosan and the carboxyl group of drug (Jeong et al., 2006).

Furthermore, the kinetics of drug delivery was investigated using semi-empirical models. More detailed mathematical models could be used in order to elucidate the exact drug release mechanism, though this probably would require additional experimental data. In order to identify the kinetic parameters, data reported in Figs. 9–12 were re-evaluated in order to be presented

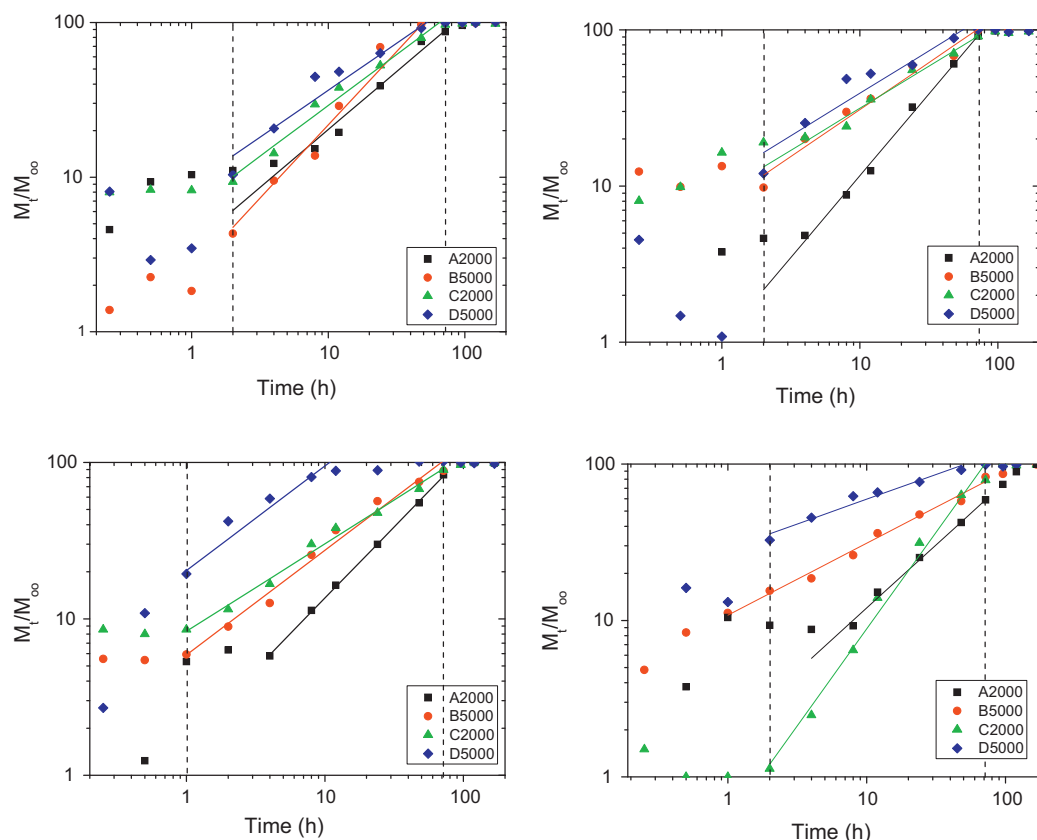


**Fig. 13.** Plots of  $M_t/M_\infty$  versus time for the samples A2000, B5000, C2000 and D5000 at 0.5 (a), 1.0 (b), 1.5 (c) and 2 (d).



**Table 2**  
Kinetic rate constants and release exponent according to Eq. (4) for all formulations.

Sample code	Initial drug released (%)	Linear region (h)	k	n	R <sup>2</sup>
A2000 0.5	10	2–72	3.63	0.75	0.998
A2000 1.0	4	4–72	1.05	1.05	0.997
A2000 1.5	5.5	4–72	1.67	0.91	0.999
A2000 2.0	9	4–72	1.87	0.81	0.998
B5000 0.5	2	2–72	2.14	1.02	0.989
B5000 1.0	11	2–72	7.76	0.60	0.987
B5000 1.5	5.5	2–72	5.89	0.67	0.992
B5000 2.0	5	1–72	10.8	0.46	0.996
C2000 0.5	8.5	2–72	6.4	0.66	0.991
C2000 1.0	12	2–72	9.12	0.54	0.989
C2000 1.5	8.5	2–72	8.32	0.56	0.985
C2000 2.0	1.0	2–72	3.24	1.14	0.994
D5000 0.5	6	2–72	9.0	0.61	0.967
D5000 1.0	4.5	2–72	11.2	0.54	0.958
D5000 1.5	4	0.5–12	20.4	0.67	0.978
D5000 2.0	10	2–72	20.9	0.42	0.979

in the usual form of  $M_t/M_\infty$  versus time. The symbols  $M_t$  and  $M_\infty$  denote cumulative amount of drug released at time  $t$  and infinite time, respectively. These data are plotted in Fig. 13a–d. For kinetic reasons in all different experimental conditions three distinctive regions were identified. The first, where the amount presents an initial high and rather constant value is attributed to the initial burst effect described previously. This period, as it can be clearly seen in these figures, lasts for approximately 2 h in most formulations, except for A2000 1, A2000 1.5 and A2000 2 where it lasts for 4 h (Table 2). The initial amount released is at most 10–11%. In the second stage lasting almost until 72 h in most samples, a linear dependence of  $M_t/M_\infty$  versus time appears when plotted in a log–log scale. In this interval, the well-known, so-called Peppas equation, or power law (Siepmann and Siepmann, 2008) was applied according to Eq. (4):

$$\frac{M_t}{M_\infty} = k \times t^n \quad (4)$$

Here,  $k$  is a constant incorporating structural and geometric characteristics of the system and  $n$  is the release exponent, which might be indicative of the mechanism of drug release. This is a very frequently used and easy-to-apply model to describe drug release which is a short time approximation of the exact solution of Fick's second law. A release exponent of 0.5 in Eq. (4) for thin films or 0.43 for spheres, as those used in this investigation, can serve as an indication for diffusion-controlled drug release. If polymer swelling is the solely release rate controlling mechanism and in the case of a delivery system with film geometry, zero order drug release kinetics are observed corresponding to a release exponent of  $n = 1$ . The corresponding value of  $n$  for spheres is equal to 0.85 (Siepmann and Siepmann, 2008). Then according to the values obtained from simulation to experimental data, only B5000 2 and D5000 2 seem to obey Fickian diffusion. Polymer swelling seems to be the main drug release mechanism in A2000 1, A2000 1.5, B5000 0.5 and C2000 2, while in all the rest samples a so-called 'anomalous' transport was observed with release exponent ranging in between 0.43 and 0.85. This is an indication of overlapping of different types of phenomena, potentially including drug diffusion and polymer swelling.

Finally, for time periods higher than 72 h a plateau is reached with the amount of drug released reaching its final constant value.

#### 4. Conclusions

PEG grafted into chitosan backbone was easefully prepared using Borch reduction process, as was verified by NMR and FTIR spectroscopy. The grafted percent is 43% for PEG2000 and 75% for

PEG5000. These materials are able to prepare nanoparticles via ionically crosslinking procedure, using TPP and PGA as crosslinking agents, in the presence of BSA, as macromolecular model drug. TPP due to its high reactivity produces nanoparticles with lower particle sizes, compared to PGA. The release profiles of BSA from grafted chitosan nanoparticles reveal that the PEG content as well as the crosslinking agent used and the crosslinking ratio determines the rate of release. Longer PEG chain as well as greater degree of substitution leads to faster drug release from nanoparticles. TPP seems to have the ability to create a more stable network leading to a slower burst effect regardless the nanoparticle size, which is smaller in comparison with the nanoparticles prepared with the use of PGA, while increasing degree of ionic crosslinking, regardless the agent used, eventually increases the release rate of BSA.

#### References

- Aktas, Y., Andrieux, K., Alonso, M.J., Calvo, P., Gürsoy, R.N., Couvreur, P., Çapana, Y., 2005. Preparation and in vitro evaluation of chitosan nanoparticles containing a caspase inhibitor. *Int. J. Pharm.* 298, 378–383.
- Amidi, M., Mastrobattista, E., Jiskoot, W., Hennink, W.E., 2010. Chitosan-based delivery systems for protein therapeutics and antigens. *Adv. Drug Deliv. Rev.* 62, 59–82.
- Bhattarai, N., Ramay, H.R., Gunn, J., Matsen, F.A., Zhang, M., 2005. PEG-grafted chitosan as an injectable thermosensitive hydrogel for sustained protein release. *J. Control. Release* 103, 609–624.
- Csaba, N., Köping-Höggård, M., Fernandez-Megia, E., Novoa-Carballal, R., Riguera, R., Alonso, M.J., 2009. Ionically crosslinked chitosan nanoparticles as gene delivery systems: Effect of PEGylation degree on in vitro and in vivo gene transfer. *J. Biomed. Nanotech.* 5, 162–171.
- Dash, M., Chiellini, F., Ottenbrite, R.M., Chiellini, E., 2011. Chitosan – A versatile semi-synthetic polymer in biomedical applications. *Prog. Polym. Sci.* 36, 981–1014.
- Deng, L., Qi, H., Yao, C., Feng, M., Dong, A., 2007. Investigation of the properties of methoxy poly(ethylene glycol)/chitosan graft co-polymers. *J. Biomater. Sci. Polym. Ed.* 18, 1575–1589.
- Gorochovceva, N., Naderi, A., Dedinaite, A., Makuska, R., 2005. Chitosan-N-poly(ethylene glycol) brush copolymers: Synthesis and adsorption on silica surface. *Eur. Polym. J.* 41, 2653–2662.
- Hajdu, I., Bodnár, M., Filipcsei, G., Hartmann, J.F., Daróczy, L., Zrínyi, M., Borbély, J., 2008. Nanoparticles prepared by self-assembly of chitosan and poly-γ-glutamic acid. *Colloid. Polym. Sci.* 286, 343–350.
- Hamidi, M., Azadi, A., Rafiei, P., 2008. Hydrogel nanoparticles in drug delivery. *Drug Deliv. Rev.* 60, 1638–1649.
- Harris, J.M., Struck, E.C., Case, M.G., Paley, M.S., Vanalstine, J.M., Brooks, D.E., 1984. Synthesis and characterization of poly(ethylene glycol) derivatives. *J. Polym. Sci. Polym. Chem. Ed.* 22, 341–352.
- Howard, K.A., 2009. Delivery of RNA interference therapeutics using polycation-based nanoparticle. *Adv. Drug Deliv. Rev.* 61, 710–720.
- Imoto, T., Kida, T., Matsusaki, M., Akashi, M., 2010. Preparation and unique pH-responsive properties of novel biodegradable nanocapsules composed of poly(g-glutamic acid) and chitosan as weak polyelectrolytes. *Macromol. Biosci.* 10, 271–277.
- Jeong, Y.I., Kim, S.H., Jung, T.Y., Kim, I.Y., Kang, S.S., Jin, Y.H., Ryo, H.H., Sun, H.S., Jin, S., Kim, K.K., Ahn, K.Y., Jung, S., 2006. Polyion complex micelles composed of all-trans retinoic acid and poly(ethylene glycol)-grafted-chitosan. *J. Pharm. Sci.* 95, 2348–2360.
- Keresztessy, Z., Bodnár, M., Ber, E., Hajdu, I., Zhang, M., Hartmann, J.F., Minko, T., Borbély, J., 2009. Self-assembling chitosan/poly-γ-glutamic acid nanoparticles for targeted drug delivery. *Colloid. Polym. Sci.* 287, 759–765.
- Lin, Y.H., Chung, C.K., Chen, C.T., Liang, H.F., Chen, S.C., Sung, H.W., 2005. Preparation of nanoparticles composed of chitosan/poly-gamma-glutamic acid and evaluation of their permeability through Caco-2 cells. *Biomacromolecules* 6, 1104–1112.
- Lin, Y.H., Mi, F.L., Chen, C.T., Chang, W.C., Peng, S.F., Liang, H.F., Sung, H.W., 2007. Preparation and characterization of nanoparticles shelled with chitosan for oral insulin delivery. *Biomacromolecules* 8, 146–152.
- Liu, Z., Jiao, Y., Wang, Y., Zhou, C., Zhang, Z., 2008. Polysaccharides-based nanoparticles as drug delivery systems. *Adv. Drug Deliv. Rev.* 60, 1650–1662.
- Markwell, M.A.K., Haas, S.M., Bieber, L.L., Tolbert, N.E., 1978. Modification of Lowry procedure to simplify protein determination in membrane and lipoprotein samples. *Anal. Biochem.* 87, 206–210.
- Muslim, T., Morimoto, M., Saimoto, H., Okamoto, Y., Minami, S., Shigemasa, Y., 2001. Synthesis and bioactivities of poly(ethylene glycol)-chitosan hybrids. *Carbohydr. Polym.* 46, 323–330.
- Nikiforidis, C.V., Kiosseoglou, V., 2010. Competitive displacement of oil body surface proteins by Tween 80 – Effect on physical stability. *Food Hydrocol.* 1–6.
- Nunthanid, J., Puttipatkhachorn, S., Yamamoto, K., Peck, G.E., 2001. Physical properties and molecular behavior of chitosan films. *Drug. Dev. Ind. Pharm.* 27, 143–157.

- Papadimitriou, S., Bikiaris, D., 2009. Novel self-assembled core-shell nanoparticles based on crystalline amorphous moieties of aliphatic copolyesters for efficient controlled drug release. *J. Control. Release* 138, 177–184.
- Papadimitriou, S., Bikiaris, D., Avgoustakis, K., Karavas, E., Georgarakis, M., 2008. Chitosan nanoparticles loaded with dorzolamide and pramipexole. *Carbohydr. Polym.* 73, 44–54.
- Park, J.H., Saravanakumar, G., Kim, K., Kwon, I.C., 2010. Targeted delivery of low molecular drugs using chitosan and its derivatives. *Adv. Drug Deliv. Rev.* 62, 28–41.
- Peng, S.F., Yang, M.J., Su, C.J., Chen, H.L., Lee, P.W., Wei, M.C., Sung, H.W., 2009. Effects of incorporation of poly(g-glutamic acid) in chitosan/DNA complex nanoparticles on cellular uptake and transfection efficiency. *Biomaterials* 30, 1797–1808.
- Rao, J.P., Geckeler, K.E., 2011. Polymer nanoparticles: preparation techniques and size-control parameters. *Prog. Polym. Sci.* 36, 887–913.
- Shu, S., Zhang, X., Teng, D., Wang, Z., Li, C., 2009. Polyelectrolyte nanoparticles based on water-soluble chitosan–poly (L-aspartic acid)–polyethylene glycol for controlled protein release. *Carbohydr. Res.* 344, 1197–1204.
- Siepmann, J., Siepmann, F., 2008. Mathematical modeling of drug delivery. *Int. J. Pharm.* 364, 328–343.
- Sonaje, K., Lin, K.J., Wang, J.J., Mi, F.L., Chen, C.T., Juang, J.H., Sung, H.W., 2010. Self-assembled pH-sensitive nanoparticles: a platform for oral delivery of protein drugs. *Adv. Funct. Mater.* 20, 3695–3700.
- Sugimoto, M., Morimoto, M., Sashiva, H., Saimoto, H., 1998. Preparation and characterization of water-soluble chitin and chitosan derivatives. *Carbohydr. Polym.* 36, 49–59.
- Tang, D.W., Yu, S.H., Ho, Y.C., Mi, F.L., Kuo, P.L., Sung, H.W., 2010. Heparinized chitosan/poly(g-glutamic acid) nanoparticles for multi-functional delivery of fibroblast growth factor and heparin. *Biomaterials* 31, 9320–9332.
- Tsao, C.T., Chang, C.H., Lin, Y.Y., Wu, M.F., Wang, J.L., Young, T.H., Han, J.L., Hsieh, K.H., 2011. Evaluation of chitosan/ $\gamma$ -poly(glutamic acid) polyelectrolyte complex for wound dressing materials. *Carbohydr. Polym.* 84, 812–819.
- Werle, M., Tacheuchi, H., Bernkop-Schnurch, A., 2009. Modified chitosans for oral drug delivery. *J. Pharm. Sci.* 98, 1643–1656.
- Yang, X., Zhang, Q., Wang, Y., Chen, H., Zhang, H., Gao, F., Liu, L., 2008. Self-aggregated nanoparticles from methoxy poly(ethylene glycol)-modified chitosan: synthesis; characterization; aggregation and methotrexate release in vitro. *Colloids Surf. B. Biointerfaces* 61, 125–131.
- Yao, K., Peng, T., Xu, M., Yuan, C., Goosen, M.F.A., Zhang, Q., Ren, L., 1994. pH-dependent hydrolysis and drug release of chitosan/polyether interpenetrating polymer network hydrogel. *Polym. Int.* 34, 213–219.
- Yao, Z., Zhang, C., Ping, Q., Yu, L.L., 2007. A series of novel chitosan derivatives: Synthesis, characterization and micellar solubilization of paclitaxel. *Carbohydr. Polym.* 68, 781–788.
- Zhang, X.G., Teng, D.Y., Wu, Z.M., Wang, X., Wang, Z., Yu, D.M., Li, C.X., 2008a. PEG-grafted chitosan nanoparticles as an injectable carrier for sustained protein release. *J. Mater. Sci. Mater. Med.* 19, 3525–3533.
- Zhang, X.G., Zhang, H.J., Wu, Z.M., Wang, Z., Niu, H.M., Li, C.X., 2008b. Nasal absorption enhancement of insulin using PEG-grafted chitosan nanoparticles. *Eur. J. Pharm. Biopharm.* 68, 526–534.
- Zhang, N., Li, J., Jiang, W., Ren, C., Li, J., Xin, J., Li, K., 2010. Effective protection and controlled release of insulin by cationic  $\beta$ -cyclodextrin polymers from alginate/chitosan nanoparticles. *Int. J. Pharm.* 393, 212–218.